Medical Engineering and Physics 67 (2019) 11–21

Contents lists available at ScienceDirect

Medical Engineering and Physics

journal homepage: www.elsevier.com/locate/medengphy

Finite element method-based study of pedicle screw–bone connection in pullout test and physiological spinal loads

Ming Xu[a], James Yang[a,*], Isador H. Lieberman[b], Ram Haddas[b]

[a] Human-Centric Design Research Lab, Department of Mechanical Engineering, Texas Tech University, Lubbock, TX, USA
[b] Texas Back Institute, Plano, TX, USA

ARTICLE INFO

Article history:
Received 12 July 2018
Revised 21 January 2019
Accepted 2 March 2019

Keywords:
Spine fusion surgery
Finite element method
Pedicle screw
Screw pullout
Von Mises stress
Lumbar spine

ABSTRACT

Finite element (FE) method has been widely used to study the screw–bone connections. Screw threads are often excluded from the FE spine model to reduce computational cost. However, no study has been conducted to compare the effect of such simplification in the screw models on the predicting accuracy of the model. The effects of different screw–bone connection types on the overall spine biomechanics are also unknown. In this study, three different types of screw–bone connections were compared using FE simulations in this study: (1) screw and bone are not fully bonded (contact connection); (2) screw is rigidly bonded with the bone (bonded connection); and (3) simplified-geometry-rigid (SGR) connection. Screw pullout test and physiological spinal loading test were simulated for the screws in this study: (1) pullout test where the pedicle screws were inserted in polyurethane foam; and (2) physiological spinal loading test (flexion, extension, lateral bending, and axial rotation) where the screws were fused into previously-validated FE lumbar spine model. The FE spine model used in this study included L_1–L_5 spine levels and simulated major ligaments and resultant muscle forces. This study indicated that the holding capability in the screw–bone interaction is smaller and the bone and implants are subjected to larger von Mises stress (up to 44.88%) in the contact connection than those in the bonded connection. Among the four spinal loading cases tested in this study, flexion produced the highest von Mises stress in both the bone and the implants. Considerable differences were observed between simplified and non-simplified screw FE models in the von Mises stress at screw–bone contact region within spinal loading environment and the ultimate screw pullout strength in pullout test. This study concluded that both the spinal implants and the bone are subjected to higher stress immediately after the pedicle-screw-instrumented surgery and before the screw and bone are fully bonded. The screw–bone interface is less likely to fail after the screw and bone are fully bonded. SGR screw model is able to predict screw force and rod stress that are consistent with those predicted by non-simplified screw models.

1. Introduction

The pedicle screw is an important tool used during spinal fusion surgery which attaches posterior spinal fixation systems to the vertebrae. Although the spinal posterior fixation systems and surgical techniques have been constantly improved during the last two decades, post-operative failures of pedicle screw have not been fully eliminated in post-surgical subjects [1–5]. Common complications in the pedicle screw-based posterior fixation surgery includes screw breakage, screw loosening, and screw pullout [5,6]. The failures of pedicle screw may lead to loss of the fixation, culminating in pain and eventually result in revision surgeries [4,7]. Demir and Camuşcu et al. [8] reported an average hospitalization cost of over $40,000 and an average hospital stay length of more than 4 days for spinal fusion surgery. Due to the high costs of the revision surgeries, there is an increasing clinical demand for analysis of the interaction between the bone and pedicle screw and the effect of pedicle screw on the biomechanical behavior of the spine [2,6,7]. Extensive experimental studies and testing have been performed investigating and improving the performance of the pedicle screws and spinal posterior fixation systems [8–15]. Standard testing methods have also been developed to gauge the performance of pedicle screws inserted in test blocks under static and fatigue loads [9,11–12]. Although these tests can quantify the behavior of pedicle screws by reporting external parameters such as ultimate strength and fatigue life cycles, they cannot reveal information internal to

* Corresponding author.
E-mail address: james.yang@ttu.edu (J. Yang).

https://doi.org/10.1016/j.medengphy.2019.03.004
1350-4533/

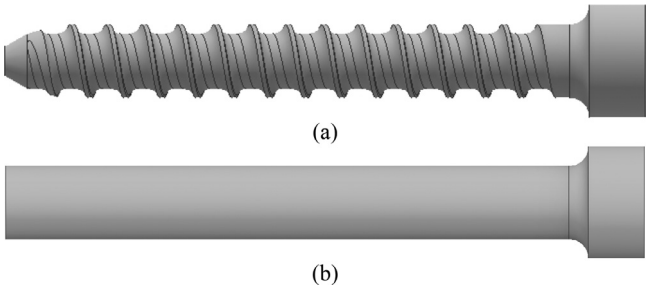

Fig. 1. Pedicle screws tested in this study: (a) non-simplified screw [7]; (b) simplified screw.

the test configurations such as the stress at the screw/test block interface, which greatly contributes to screw/bone failure [6,7]. Besides, tests using test blocks can provide very simplified and limited physiological spinal loads. Finite element analysis (FEA) can provide detailed information at the screw–bone interface and can feasibly test the pedicle screw under physiological spinal loads within spine FEA model, which has been widely used to study the biomechanics of lumbar spines instrumented with pedicle screws [9,13]. To reduce computational cost, the geometry of the pedicle screw in FEA study is often simplified (eliminating screw threads) and the screw–bone interaction is often simulated as rigid connection in most of the previous FE studies [9,13]. This type of simplified-geometry-rigid (SGR) screw–bone connection model assumes no relative movement between the bone and screw. However, the effect of simplification introduced by SGR models have not been fully reported in the literatures, where oversimplifications might occur in predicting parameters such as stress. Moreover, the screw–bone connection mechanism varies in post-surgical spines. Chazistergos et al. [2] modeled the thread of pedicle screw and claimed that the screw–bone interaction should be categorized into two scenarios from clinical observations: (1) immediately after the pedicle screw-instrument surgery, the screw and bone are not fully bonded where the relative movement and friction force between the screw and surrounding bony tissues should be considered (contact connection); (2) after the surgery for a longer period of time, the screw and bone would be fully bonded together where the relative movement between the screw and bone could be ignored (bonded connection). Chazistergos et al. [2] compared the difference between the contact connection and bonded connection of the screw–bone interface using FE simulations. Their study revealed that the stress distributions of the bone and pedicle screw predicted in contact connection and bonded connection are different. Kiapour et al. [18] also compared the bonded connection and contact connection between the pedicle screw and vertebrae. In their study, one vertebra was inserted with a pedicle screw and this instrumented vertebra was subject to simplified compressive loads. Their study found that the screw–bone contact condition has considerable effect on the load transfer in the screw–bone interface where the contact connection produces significantly higher stress in the screw than the bonded condition does. To the best of our knowledge, no previous study has been performed to investigate the effects of these above-mentioned different FEA modeling methods of screw–bone contact types on the biomechanical behavior of the spine under physiological spinal loading environment. To better understand and utilize these FEA screw–bone modeling methods, different FEA modeling methods should be tested and compared under various types of loads including physiological spinal loading conditions. This study intended to provide optimized FEA modeling methods for the screw–bone interaction and ultimately provide guidelines for future FEA studies that are designed to utilize these tested methods. The objectives of this study are: (1) to develop FE models of two different types of pedicle screws (one non-simplified screw models and one simplified screw model) and compare the predicting capability of SGR model with that of non-simplified screw models; (2) to study the effect of different types of screw–bone connection on the biomechanical performance of lumbar spine and spinal implants under physiological spinal loads using previously-validated FE spine model.

Table 1
Design variables for the non-simplified pedicle screw [7].

Thread-shank junction	Deep step
Pitch (mm)	2.8
Proximal root radius (mm)	0.8
Distal root radius (mm)	1.2
Proximal half angle (deg.)	14
Distal half angle (deg.)	25
Thread width (mm)	0.2

2. Methods

2.1. Pedicle screw FE models and validation

Computer aided design (CAD) model of one non-simplified pedicle screw was created in Autodesk Inventor® (Autodesk, San Rafael, CA, USA) based on the geometries described in the literature [7]. One geometry-simplified pedicle screw was also created to represent the SGR screw–bone connection. Both of the two screws have an identical length of 45 mm and outer diameter of 6.5 mm (Fig. 1). The design variables and specifications of the non-simplified screw were summarized in Table 1 and Fig. 2.

The CAD model of the non-simplified pedicle screw was imported into Hypermesh® (Altair Engineering, Troy, MI, USA) and

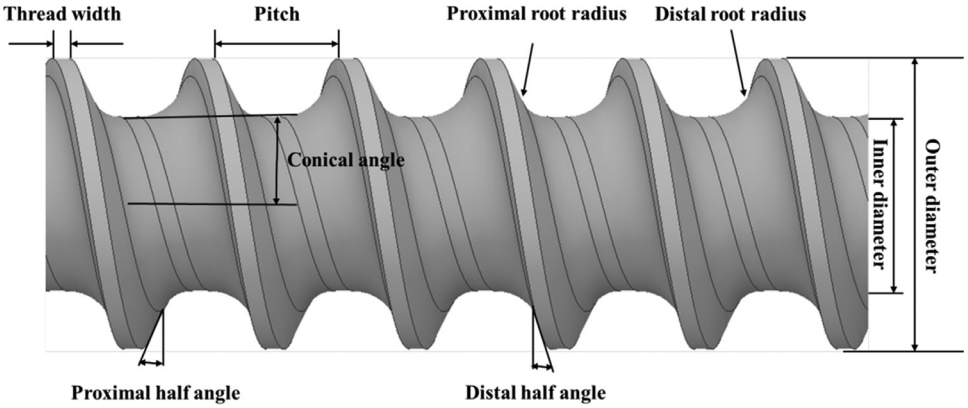

Fig. 2. Design variables of the non-simplified pedicle screw [7].

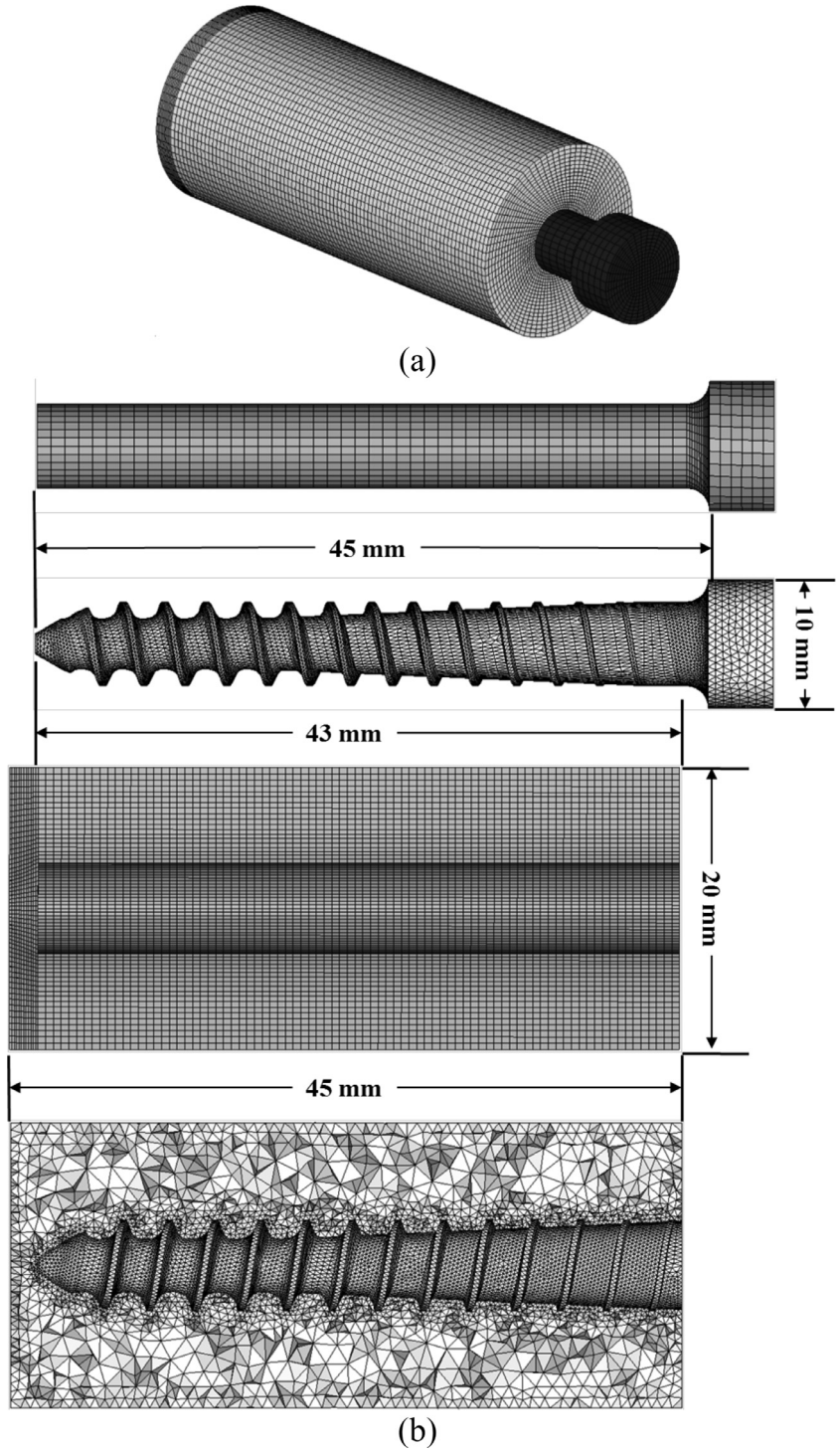

Fig. 3. FE models of the pullout test: (a) test configuration; (b) FE screw and cylinder models for non-simplified screw models (used for contact and bonded connections) and simplified screw model (used for SGR connection).

meshed with 4-node tetrahedral elements. The simplified pedicle screw was meshed into 8-node hexahedral elements using TrueGrid® (XYZ Scientific Applications, Pleasant Hill, CA, USA). For each screw, the meshed screw geometry was inserted into a cylinder model representing the polyurethane foam (Fig. 3(a)). The cylinder model has a diameter of 20 mm and a height of 45 mm [7]. Mesh refinement and mesh convergence tests were performed to determine an appropriate mesh resolution to ensure both the calculation accuracy and efficiency, where the difference of simulation results between the two sequential sets of the mesh was smaller than 5% [19]. The final element numbers selected for the ten non-simplified pedicle screws ranged from 54,413 to 74,909 and the element number selected for simplified pedicle screw is 5376 (Fig. 3(b)). The FE cylinder model contained from 171,002 to 237,384 elements when inserted with the non-simplified screws and 41,512 elements when inserted with the simplified pedicle screw (Fig. 3(b)). The polyurethane foam (Sawbones-Pacific Research Laboratories, Vashon, WA, USA) tested in this FE simulation

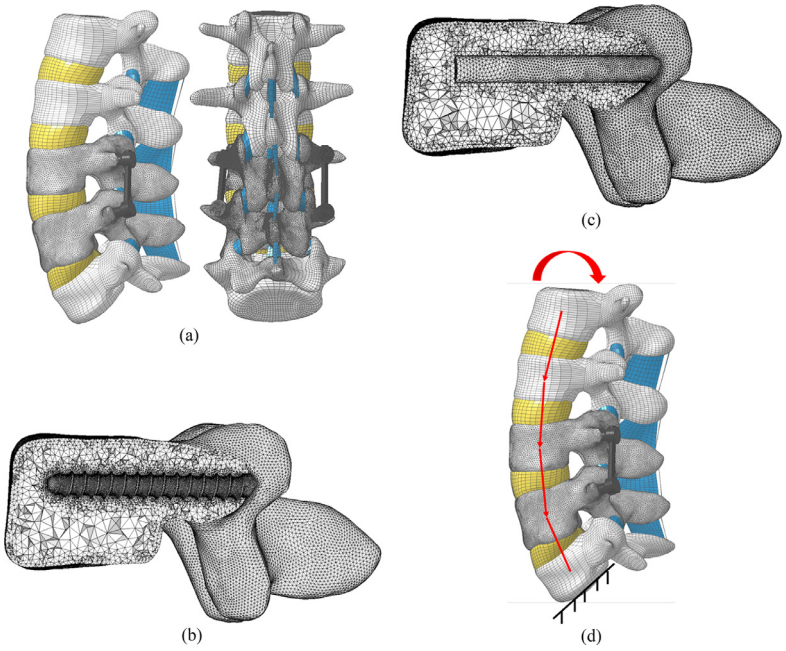

Fig. 4. Lumbar spine FE model instrumented with pedicle screws and rods: (a) model configuration with posterior and side views; (b) screw hole in vertebra when inserted with non-simplified pedicle screws; (c) screw hole in vertebra when inserted with simplified pedicle screw; and (d) loading condition (marked in red) and boundary condition (marked in black) applied in spine tests.

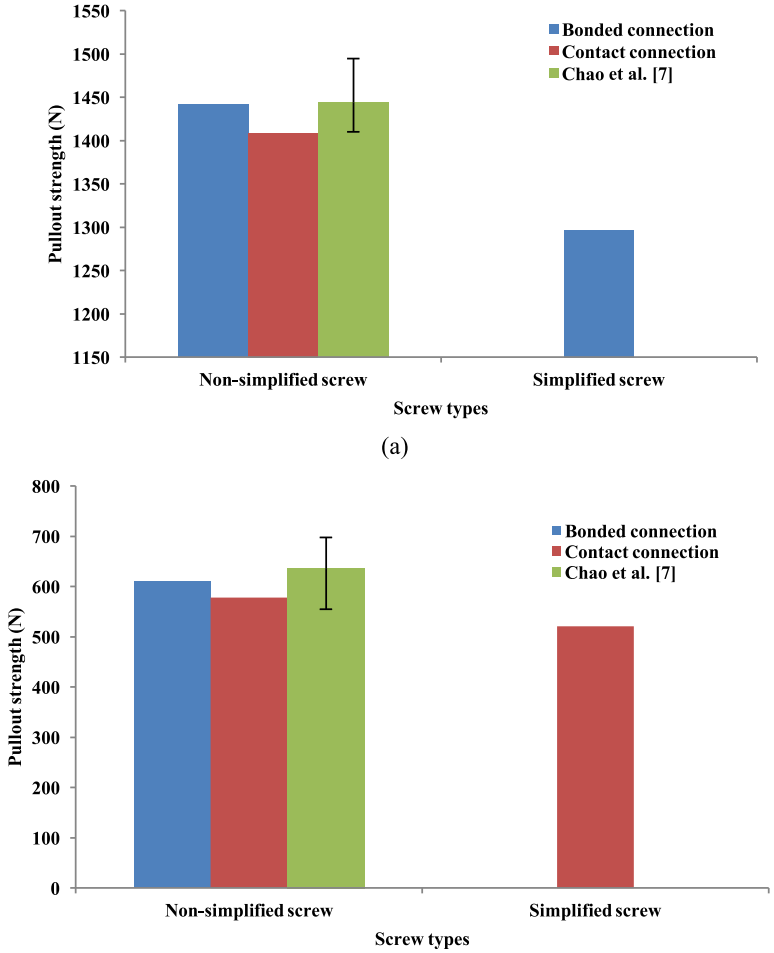

Fig. 5. Pullout strength comparison of simulations from the contact model, bonded model, and SGR model, and mechanical experiments [7]: (a) high-density foam; (b) low-density foam.

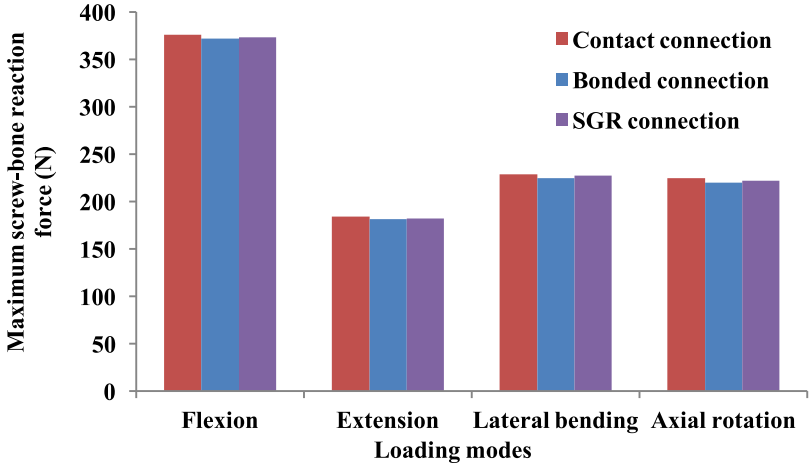

(a)

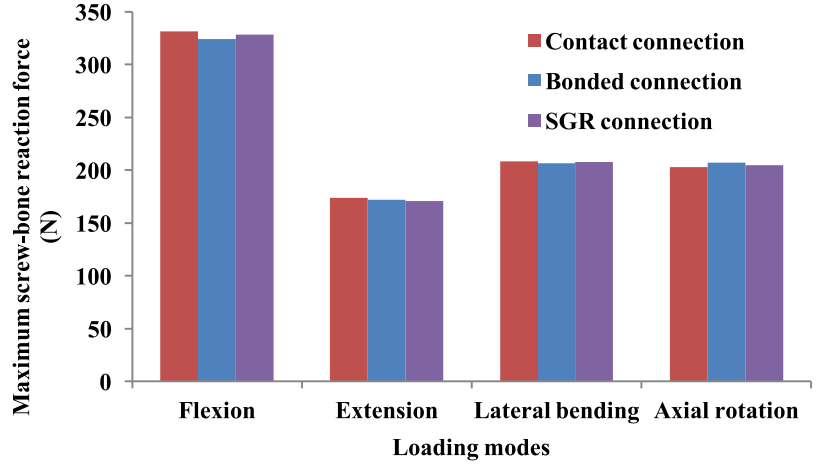

(b)

Fig. 6. Maximum screw–bone reaction forces in: (a) L_3 and (b) L_4 under physiological loading conditions.

has similar material property as human cancellous bones. Both the screws and foams simulated in this study were assumed to have homogeneous and isotropic material properties [7]. The pedicle screws have Young's modulus of 114 GPa and Poisson's ratio of 0.3 [7]. To represent bones with various densities and material properties, two types of polyurethane foam were tested for each screw. The first type of polyurethane has density of 0.16 g/mm^3, Young's modulus of 23 MPa, and yield stress of 2.3 MPa. The second type of polyurethane foam has density of 0.32 g/mm^3, Young's modulus of 137.5 MPa, and yield stress of 5.8 MPa [7]. The screws and cylinders were imported into LS-DYNA (Livermore Software Technology Corp, Livermore, CA, USA) for FE simulations. Explicit solver in LS-DYNA was utilized in this study. For the contact model, the friction coefficient between the pedicle screw and cylinder was set to 0.2 [20]. The loading condition in the FE simulation was kept consistent with the loading condition utilized in mechanical tests [7]: a axial pullout loading with a rate of 5 mm/min was applied at the screw head while the side surface of the cylinder was constrained for both translational and rotational movements. The magnitude of the axial force applied at the screw head was recorded during the pullout process. The pullout force was the axial force applied at the screw head when the pullout occurred where the sudden decrease of the pullout force was observed [20]. To validate the pedicle screw FE models, the pullout strength predicted by the contact connection was compared to the experimental results reported by Chao et al. [7]. Here only contact connection simulation was conducted to compare with the experimental results because the pedicle screw and foam were in simple contact in the pullout experiments where no bond was formed [6,7,20]. The pullout strengths predicted by the bonded connection were compared with the experimental results as well.

2.2. Pedicle screw-instrumented lumbar spine FE model and physiological loading tests

In this study, one previously-validated three-dimensional (3D) nonlinear FE model of intact lumbar spine (L_1–L_5 spinal levels, 47 years old male subject) [21] was used to provide the physiological spinal loads on the screw–bone interface. Details about the modeling methods of this employed FE lumbar spine model could be found in our previous study [21]. Each vertebra consisted of a cancellous core surrounded by a cortical shell layer with a thickness of 1 mm [22]. At both ends of each vertebra, cartilaginous endplates were simulated with a thickness of 0.8 mm [19]. The facet cartilage joints were modeled as a soft frictionless contact with

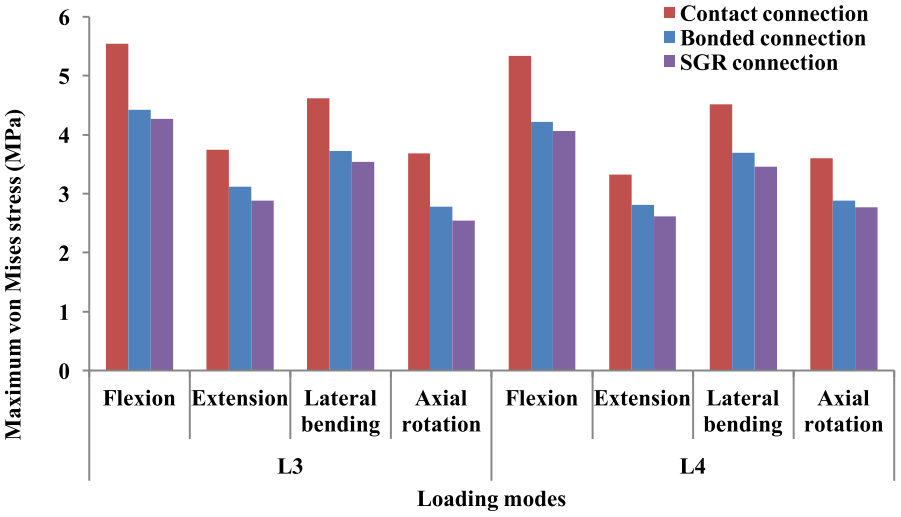

(a)

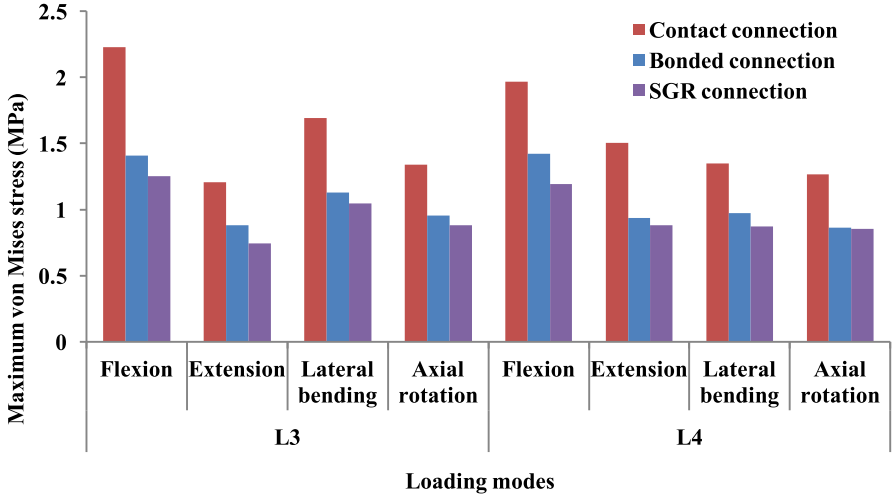

(b)

Fig. 7. Maximum von Mises stress of L_3 and L_4 cancellous obtained by contact connection and bonded connection under four physiological loading conditions: (a) high-density bone; and (b) low-density bone.

Table 2
Material properties of the lumbar spine FE model [17].

Material	Modulus (MPa)	Poisson's ratio	References
Cortical bone	12,000	0.30	[18]
Cancellous bone	100	0.20	[18]
Posterior bony elements	3500	0.25	[31]
Cartilaginous endplate	23.80	0.40	[31]
Annular ground substance	Hyperelastic (Mooney-Rivlin) c1 = 0.56, c2 = 0.14	0.45	[32]
Annular collagen fibers	Nonlinear stress-strain curve		[33]
Nucleus pulposus	Hyperelastic (Mooney-Rivlin) c1 = 0.12, c2 = 0.09	0.4999	[32]
Ligaments	Nonlinear stress-strain curves		[34]

an initial gap of 0.5 mm [22]. Seven major ligaments, i.e., anterior longitudinal ligament (ALL), posterior longitudinal ligament (PLL), flaval ligament (FL), facet capsular ligament (CL), intertransverse ligament (ITL), interspinous ligament (ISL), and supraspinous ligament (SSL), were meshed by 4-node shell elements [23]. Local muscle forces and upper body weight in lumbar spine were simulated by a compressive follower load (500 N or 1175 N) with optimized path through the vertebrae [24]. The material properties for the lumbar spine FE model were summarized in Table 2.

The spine FE model was inserted with the simplified and non-simplified screws at L_3–L_4 separately (Fig. 4(a)). The screw-inserted vertebrae were meshed by 4-node tetrahedral elements in Hypermesh ®. The rest of bony tissues in this FE model were meshed by 8-node hexahedral elements in TrueGrid ® [23,25]. Mesh convergence tests for this FE lumbar spine model were performed in our previous study [23]. The screw-inserted vertebrae contained from 259,834 to 357,136 elements when inserted with non-simplified screws and 221,762 elements when inserted with

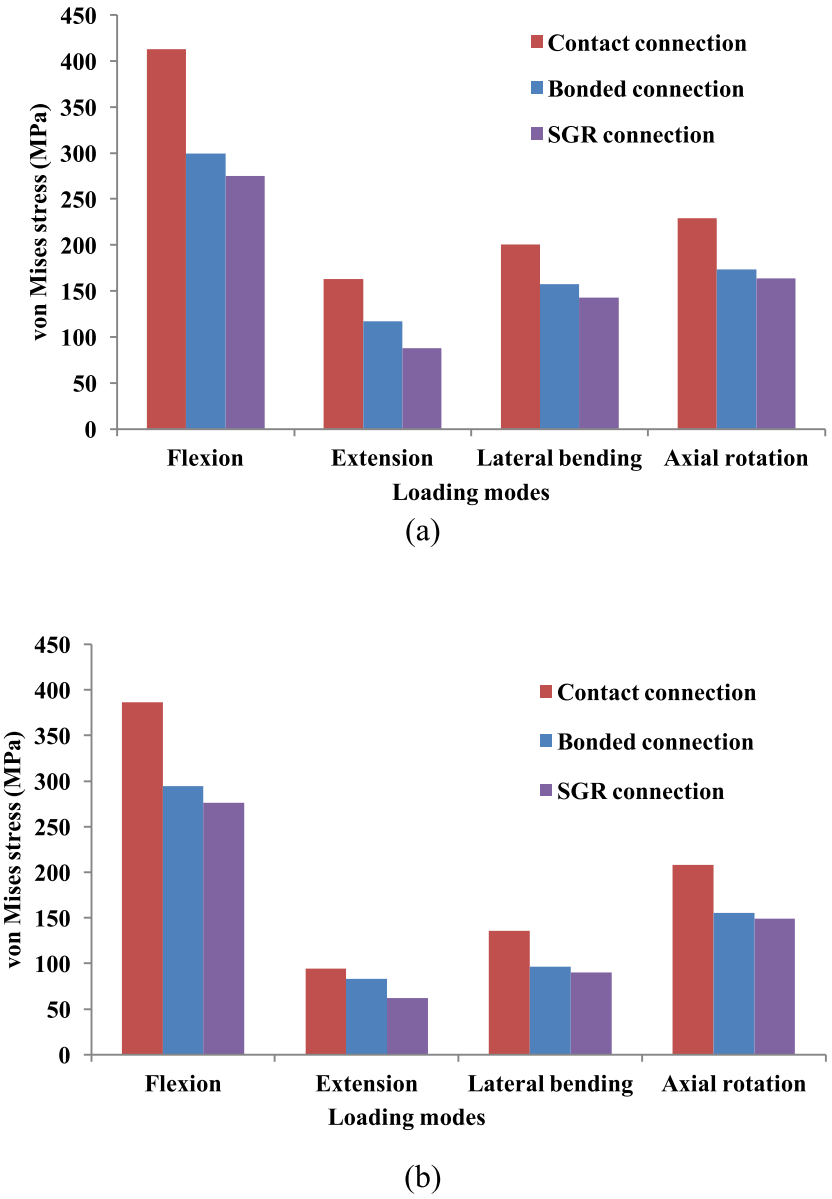

Fig. 8. Maximum von Mises stress of the pedicle screws in: (a) L_3; and (b) L_4 under four physiological loading conditions.

Table 3
Loading modes tested for the instrumented lumbar spine FE model [28].

Loading modes	Follower force (N)	Moment (Nm)
Flexion	1175	7.5
Extension	500	7.5
Lateral bending	500	7.8
Axial rotation	500	5.5

simplified screw. Rigid connections between the pedicle screws and rods were assigned in this study [26,27]. Bonded connections were assumed between the ligaments and bony tissues. Three different types of screw–bone interactions (bonded connection, contact connection, and SGR connection) were modeled and compared. This lumbar spine FE model was tested in four loading modes: flexion, extension, lateral bending, and axial rotation [28]. The detailed forces and moments for these physiological loading modes were summarized in Table 3. Maximum interaction forces between the screw and bone were recorded and compared under the four loading modes. For the bony tissues in the effective region, two sets of material properties representing high-density and low-density bones were tested and compared [7]. In addition, maximum von Mises stress in the pedicle screws and rods, and cancellous bone substitute within the effective region were recorded.

3. Results

3.1. Pedicle screw FE model validation and pullout tests

As shown in Fig. 5, the pullout strengths predicted by the contact connection, bonded connection, and SGR connection in this study were compared with experimental results [7]. For both high-density and low-density foams, we had the following results: for non-simplified screw, the pullout strength from the bonded model was larger than that from the contact model; the pullout strength of the SGR model was smaller than those of the non-simplified model and experimental test [7]; the pullout strength of the

non-simplified screws in this study matched the experimental results [7].

3.2. Pedicle screw-instrumented lumbar spine FE model

3.2.1. Screw–bone interaction forces

The screw–bone interaction forces predicted by the three types of screw–bone interactions were compared (Fig. 6). In all loading cases, the differences in predicted screw–bone forces among three types of connections were small, where maximum difference was less than 3%. Among the four loading cases, flexion produced the largest screw–bone interaction forces and the smallest interaction forces were observed in extension. In L_3, the maximum interaction forces for the four loading cases were 376 N in flexion, 183 N in extension, 228 N in lateral bending, and 224 N in axial rotation. In L_4, the maximum reaction forces for the four loading cases were 255 N in flexion, 133 N in extension, 160 N in lateral bending, and 156 N in axial rotation. The interaction forces in L_3 were larger than those in L_4: 13.5% larger in flexion, 5.9% larger in extension, 9.6% larger in lateral bending, and 8.4% larger in axial rotation.

3.2.2. von Mises stress in the cancellous bone

In both the high-density and low-density bones, contact connection produced the highest von Mises stress in the cancellous bone substitute whereas the SGR connection generated the lowest stress in the cancellous bone (Fig. 7). In the high-density bone, the percentage differences of maximum von Mises stress between those predicted by the contact connection and those predicted by SGR connection in the four loading cases were 30.04% in flexion, 30.31% in extension, 30.87% in lateral bending, and 44.88% in axial rotation. The maximum von Mises stresses predicted in the high-density bone were considerably higher than those predicted in the low-density bone in all four loading cases. Among the four loading cases, flexion produced the highest maximum von Mises stress in cancellous bone substitute, which were 5.54 MPa in the high-density bone and 2.22 MPa in the low-density bone. The maximum von Mises stresses of cancellous bone in L_3 were higher than those predicted in L_4. The In high-density bone, the percentage difference between L_3 and L_4 were 7.62% in flexion, 12.50% in extension, 2.43% in lateral bending, and 2.45% in axial rotation.

3.2.3. von Mises stress of the pedicle screws

As shown in Fig. 8, flexion produced the highest maximum von Mises stress among the four loading modes wheras extension produced the lowest. The maximum von Mises stresses of the pedicle screws in L_3 were higher than those in L_4 in each loading direction. Among the three screw–bone connection types tested in this study, the SGR connection produced the lowest von Mises stress in the pedicle screws for all the loading cases in both L_3 and L_4 wheras the contact connection had the highest.

As shown in Fig. 9, the von Mises stress in the pedicle screws concentrated on the screw shank/body junction areas under all the loading conditions.

3.2.4. von Mises stress of the rods

As shown in Fig. 10, the three types of screw–bone connections predicted comparable von Mises stress in the rods, where the difference was less than 1%. The maximum von Mises stress occurred in the flexion loading case were the largest and in extension the maximum von Mises stress were the smallest. The simulated maximum von Mises stress values were 391. 42 MPa in flexion, 96.76 MPa in extension, 226.19 MPa in lateral bending, and 244.28 MPa in axial rotation.

As shown in Fig. 11, the highest von Mises stress occurred at the screw–rod connecting area under all the loading conditions, which was consistent with the clinical observations [16] and experimental tests [14].

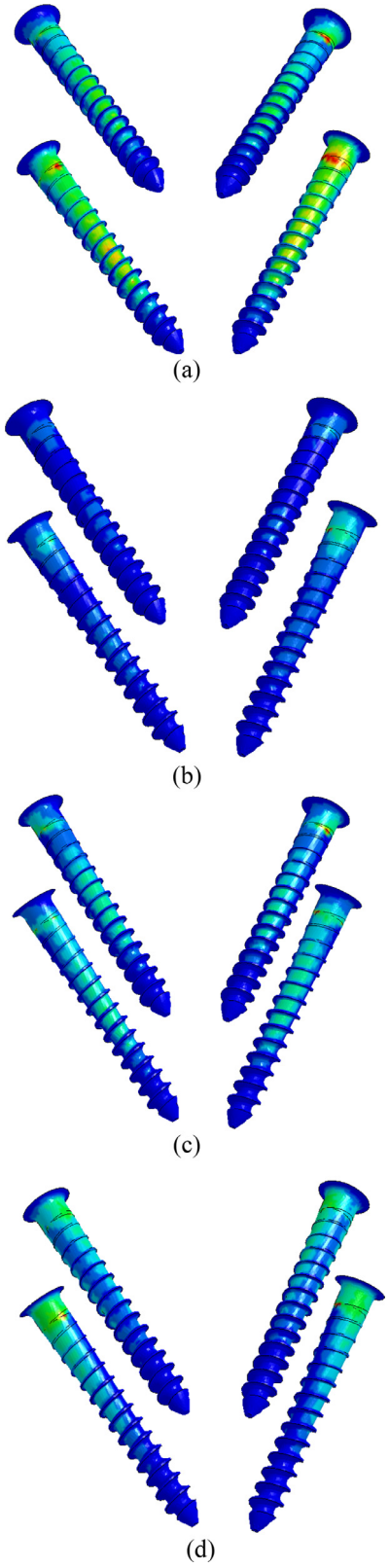

Fig. 9. Contour plots of von Mises stress in the pedicle screws with contact connection model (color bar: 0–450 MPa, anterior-superior view) under: (a) flexion; (b) extension; (c) lateral bending; and (d) axial rotation.

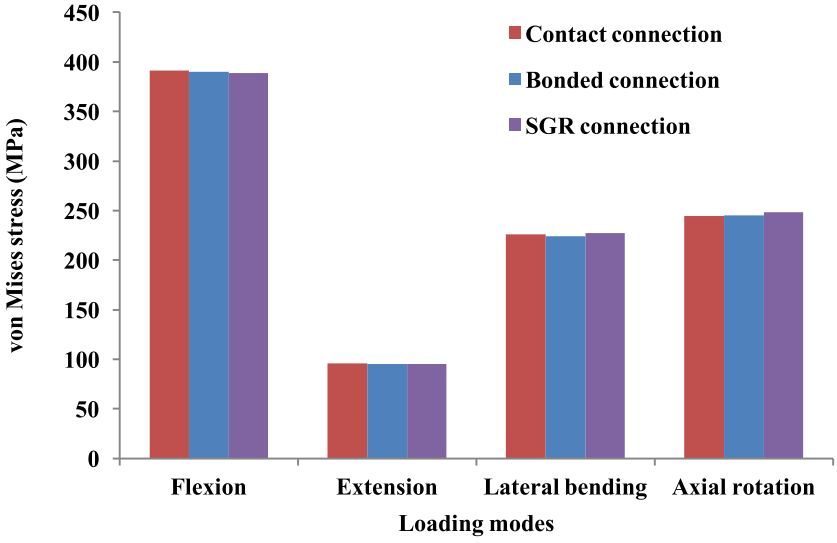

Fig. 10. Maximum von Mises stress of the rods under four physiological loading conditions.

4. Discussion

This study compared three different screw–bone connections. The pullout strength predicted by the FE simulations in this study matched well with the experimental results reported by [7], which validated the screw–bone FE models developed in this study.

The bonded connection provided larger pullout strengths than the contact models. This suggested that the failure at the screw–bone interface is more likely to occur right after the pedicle-screw-instrumented surgery. The SGR model could be considered as a special case in bonded model where the thread depth was zero. This was the reason why SGR model predicted smaller pullout strength than those predicted by the non-simplified screw models and the experimental test. However, in the spinal loading test where the screw–bone reaction force is far from reaching the pullout limit of the pedicle screw, SGR connection is an efficient and qualified simplification, which is widely used in FE spine models in the literatures [19–23].

The von Mises stress in both the pedicle screws and the vertebrae predicted by the SGR connection was lower than those predicted by contact connection and bonded connection. This was due to the fact that no screw thread was simulated in SGR model, which reduced the stress concentration in the screw. Thus, the SGR model was not the proper option to simulate the maximum von Mises stress at the screw–bone contact region. To simulate the stress distribution at the screw–bone contact region, screw thread should be considered. The maximum von Mises stresses predicted by the contact connection were higher than those predicted by the bonded connection under identical loading conditions, which was consistent with the results reported by Chao et al. [7]. This suggested that both the spinal implants and the bone are subjected to higher stress immediately after the pedicle-screw-instrumented surgery. The screw–bone interface is more stable after the screw and bone are fully bonded. Based on the screw–bone reaction force and von Mises stress in the bone, bone fracture and screw loosening is most likely to occur under flexion among the four tested loading modes in this study [22].

The screw–bone interaction forces predicted by the three types of screw–bone connections were close under all four loading cases, which is consistent with the mechanical fundamental that the reaction force between two contact surfaces is irrelevant with the geometry of the contact area. This suggested that the SGR connection is able to accurately predict the screw–bone reaction force under the condition that the screw and bone fully bonded together. The simplified screw model have limited effect on the external biomechanicl hehavior of the spine model (range of motion, etc.) after the screw and bone are fully bonded. The von Mises stress of the rod is also not affected by the modeling method of the screw–bone interface. This is consistent with the findings in the literatures [19–23]. Thus, when predicting the overall biomechanical behavior of the spine without concerning the failure in the screw–bone interface, eliminating the screw thread from the model is an efficient and safe simplification. The highest von Mises stress concentrated on the shank/body junction area in the pedicle screw under all the loading conditions. The highest von Mises stress in the rod concentrated at the connecting areas with the screws. These two predictions were consistent with the clinical observations and experimetnal tests, which furthur validated the screw FEA models in this study.

This study identified the limitations and advantages of the three types of screw/bone connection models. For the simplified SGR model, it has advantages in greatly reducing the simulation time and can provide acceptable predicting results when it comes to simulating the force and displacement of the spine models. Thus, SGR model can be integrated in the future simulation-based surgical planning tool and spine FEA model for force and displacement prediction. By comparing the bonnded and contact screw/bone connection models, this study was able to show that greater risk of screw pullout and loosening failures might occur before the screw and bone are fully fused together after the surgery. Thus, large loads on the screws and spine should be avoided immediately after the surgery.

In this study, only static loading conditions were tested in the pullout test and the spine model. However, long-term fatigue damage accumulation in the screw–bone interaction also greatly contributes to the screw failure and screw loosening [29]. In fact, fatigue failure of the spinal implants is more commonly observed in post-surgical subjects than the immediate implant failure which is normally caused by sudden large amount of load on the implants [30]. In our future work, long-term fatigue behavior of the screw–bone connections will be studied.

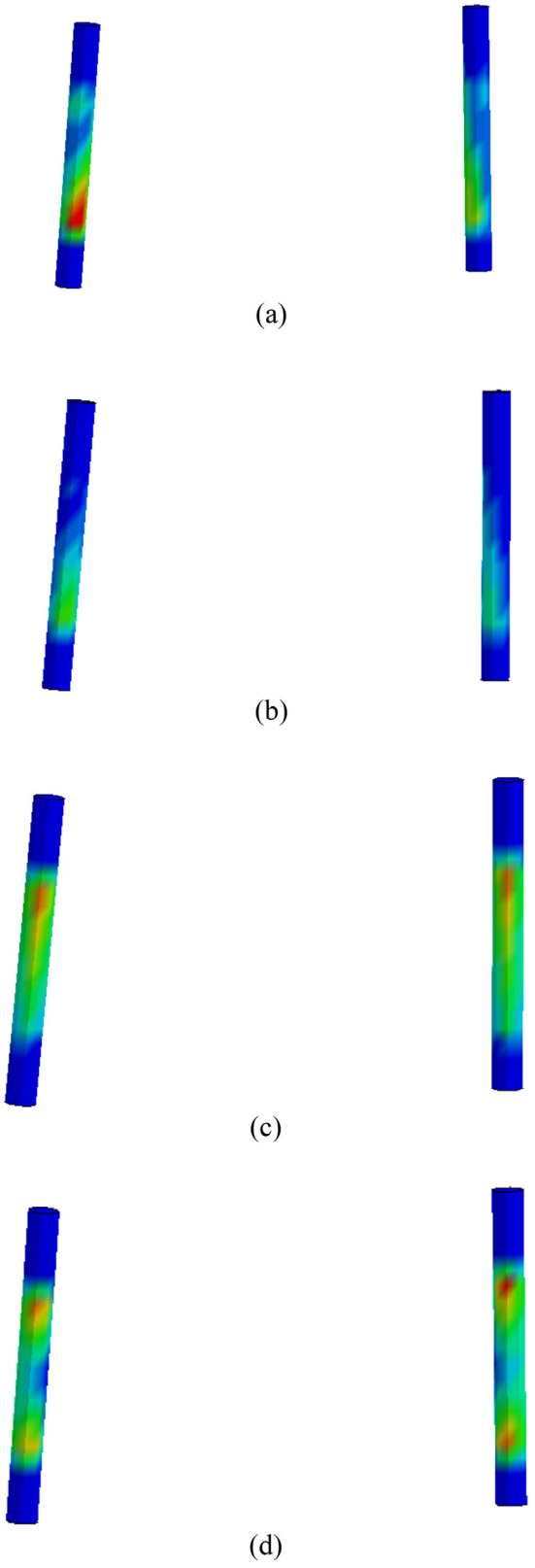

Fig. 11. Contour plots of von Mises stress in the rods (color bar: 0–400 MPa, posterior view) with contact connection model under: (a) flexion; (b) extension; (c) lateral bending; and (d) axial rotation.

5. Conclusion

This study investigated three different ways of screw–bone connection in finite element model and results showed that both the spinal implants and the bone are subjected to higher stress right after the pedicle-screw-instrumented surgery. The screw–bone interface is less likely to fail after the screw and bone are fully bonded. Simplified screw models excluding the screw thread can predict screw force and rod stress consistent with those predicted by models including the screw thread.

Acknowledgments

This work was partly supported by NSF project (Award #: 1703093).

Competing interests

None declared.

Ethical approval

Not required.

References

[1] Amaritsakul Y, Chao CK, Lin J. Biomechanical evaluation of bending strength of spinal pedicle screws, including cylindrical, conical, dual core and double dual core designs using numerical simulations and mechanical tests. Med Eng Phys 2014;36(9):1218–23.
[2] Chazistergos P, Ferentinos G, Magnissalis A, Kourkoulis SK. The pull-out strength of transpedicular screws in posterior spinal fusion. In: Paper presented at: sixteenth European conference of fracture, Alexandroupolis, Greece; 2006.
[3] Chao KH, Lai YS, Chen WC, Chang CM, McClean CJ, Fan CY, Chang CH, Lin LC, Cheng CK. Biomechanical analysis of different types of pedicle screw augmentation: a cadaveric and synthetic bone sample study of instrumented vertebral specimens. Med Eng Phys 2013;35(10):1506–12.
[4] Elder BD, Holmes SL, Goodwin C, Kosztowski TA, Lina IA, Locke JE, Witham TF. The biomechanics of pedicle screw augmentation with cement. Spine J 2015;15(6):1432–45.
[5] Chen CS, Chen WJ, Cheng CK, Jao SHE, Chueh SC, Wang CC. Failure analysis of broken pedicle screws on spinal instrumentation. Med Eng Phys 2005;27(6):487–96.
[6] Liu S, Qi W, Zhang Y, Wu Z-X, Yan Y-B, Lei W. Effect of bone material properties on effective region in screw–bone model: an experimental and finite element study. Biomed Eng Online 2014;13(83):1–13.
[7] Chao C-K, Hsu C-C, Wang J-L, Lin J. Increasing bending strength and pull-out strength in conical pedicle screws: biomechanical tests and finite element analyses. J Spinal Disord Tech 2008;21(2):130–8.
[8] Demir T, Camuşcu N. Design and performance of spinal fixation pedicle screw system. Proc Inst Mech Eng H 2012;226:33–40.
[9] La Barbera L, Ottardi C, Villa T. Comparative analysis of international standards for the fatigue testing of posterior spinal fixation systems: the importance of preload in ISO 12189. Spine J 2015;15:2290–6.
[10] Kovacı H, Yetim AF, Çelik A. Biomechanical analysis of spinal implants with different rod diameters under static and fatigue loads: an experimental study. Biomed Eng/Biomed Tech 2018.
[11] Villa T, La Barbera L, Galbusera F. Comparative analysis of international standards for the fatigue testing of posterior spinal fixation systems. Spine 2014;14:695–704.
[12] La Barbera L, Galbusera F, Villa T, Costa F, Wilke H-J. ASTM F1717 standard for the preclinical evaluation of posterior spinal fixators: can we improve it? Proc Inst Mech Eng H 2014;228:1014–26.
[13] La Barbera L, Galbusera F, Wilke H-J, Villa T. Preclinical evaluation of posterior spine stabilization devices: can the current standards represent basic everyday life activities? Eur Spine J 2016;25:2909–18.
[14] La Barbera L, Villa T. Toward the definition of a new worst-case paradigm for the preclinical evaluation of posterior spine stabilization devices. Proc Inst Mech Eng H 2017;231:176–85.
[15] Boero Baroncelli A, Reif U, Bignardi C, Peirone B. Effect of screw insertion torque on push-out and cantilever bending properties of five different angle-stable systems. Vet Surg 2013;42(3):308–15.
[16] Martin BI, Franklin GM, Deyo RA, Wickize TM, Lurie JD, Mirza SK. How do coverage policies influence practice patterns, safety, and cost of initial lumbar fusion surgery? A population-based comparison of workers' compensation systems. Spine J 2014;14(7):1237–46.

[17] Goel VK, Kiapour A, Faizan A, Krishna M, Friesem T. Finite element study of matched paired posterior disc implant and dynamic stabilizer (360° motion preservation system). SAS J 2007;1(1):55–61.
[18] Kiapour A, Ambati D, Hoy RW, Goel VK. Effect of graded facetectomy on biomechanics of dynesys dynamic stabilization system. Spine 2012;37(10):E581–9.
[19] Rohlmann A, Burra NK, Zander T, Bergmann G. Comparison of the effects of bilateral posterior dynamic and rigid fixation devices on the loads in the lumbar spine: a finite element analysis. Eur Spine J 2007;16(8):1223–31.
[20] Rohlmann A, Boustani HN, Bergmann G, Zander T. Effect of a pedicle-screw-based motion preservation system on lumbar spine biomechanics: a probabilistic finite element study with subsequent sensitivity analysis. J Biomech 2010;43(15):2963–9.
[21] Ambati DV, Wright EK Jr, Lehman RA Jr, Kang DG, Wagner SC, Dmitriev AE. Bilateral pedicle screw fixation provides superior biomechanical stability in transforaminal lumbar interbody fusion: a finite element study. Spine J 2015;15(8):1812–22.
[22] Chen SI, Lin RM, Chang CH. Biomechanical investigation of pedicle screw-vertebrae complex: a finite element approach using bonded and contact interface conditions. Med Eng Phys 2003;25(4):275–82.
[23] Ayturk UM, Puttlitz CM. Parametric convergence sensitivity and validation of a finite element model of the human lumbar spine. Comput Methods Biomech Biomed Eng 2011;14(8):695–705.
[24] Hashemi A, Bednar D, Ziada S. Pullout strength of pedicle screws augmented with particulate calcium phosphate: an experimental study. Spine J 2009;9(5):404–10.
[25] Xu M, Yang J, Lieberman IH, Haddas R. Lumbar spine finite element model for healthy subjects: development and validation. Comput Methods Biomech Biomed Eng 2016;20(1):1–15.
[26] Zander T, Rohlmann A, Bergmann G. Influence of different artificial disc kinematics on spine biomechanics. Clin Biomech 2009;24:135–42.
[27] Bowden AE, Guerin HL, Villarraga ML, Patwardhan AG, Ochoa JA. Quality of motion considerations in numerical analysis of motion restoring implants of the spine. Clin Biomech 2008;23(5):536–44.
[28] Dreischarf M, Zander T, Bergmann G, Rohlmann A. A non-optimized follower load path may cause considerable intervertebral rotations. J Biomech 2010;43(13):2625–8.
[29] Li CQ, Zhou Y, Wang HW, Liu J, Xiang LB. Treatment of unstable thoracolumbar fractures through short segment pedicle screw fixation techniques using pedicle fixation at the level of the fracture: a finite element analysis. PLoS One 2014;9(6).
[30] Brasiliense LBC, Lazaro BCR, Reyes PM, Newcomb A, Turner JL, Crandall DG, Crawford NR. Characteristics of immediate and fatigue strength of a dual-threaded pedicle screw in cadaveric spines. Spine J 2013;13(8):947–56.
[31] Lu Y, Hutton W, Gharpuray V. Do bending, twisting, and diurnal fluid changes in the disc affect the propensity to prolapse? A viscoelastic finite element model. Spine 1996;21:2570–9.
[32] Schmidt H, Galbusera F, Rohlmann A, Shirazi-Adl A. What have we learned from finite element model studies of lumbar intervertebral disc in the past four decades. J Biomech 2013;46:2342–55.
[33] Shirazi-Adl A, Ahmed A, Shrivastava S. Mechanical response of a lumbar motion segment segment in axial torque alone and combined with compression. Spine 1986;11(9):914–27.
[34] Eberlein R, Holzapfel G, Frohlich M. Multi-segment FEA of the human lumbar spine including the heterogeneity of the annulus fibrosus. Comput Mech 2004;34:147–63.